Optimal Method for Preparation of Magnetite Nanoparticles

[1]UMAR SAEED KHAN*, [2]NAZIR SHAH KHATTAK,
[3]AMINUR RAHMAN AND [3]FARIDULLAH KHAN
[1]*Institute of Physics & Electronics, University of Peshawar, Peshawar, Pakistan.*
omar_aps@yahoo.co.uk*
[2]*Dean of Sciences, Sarhad University of Sciences and Information Technology, Peshawar, Pakistan.*
[3]*Pakistan Council of Scientific and Industrial Research Labs complex, Peshawar, Pakistan.*

Summary: This paper deals with the synthesis and characterization of magnetite nanoparticles via the controlled modified chemical coprecipitation method using ferrous and ferric salt solution in alkaline medium with out any surfactant addition. The nanoparticles of 9–14 nm in size were prepared under non-oxidized environment and characterized by transmission electron microscopy, energy dispersive X-rays spectrometry, X-ray diffraction and BET surface area analyzer. The reaction temperature and the stirring rate during the precipitation were found to be crucial in limiting their size and size distribution. Low temperature and high stirring rate are the appropriate conditions for the synthesis of these particles.

Introduction

The utilization of magnetic nanoparticles has been an active field of science and technology due to its potential applications in different disciplines such as biomedicine [1], biomedical diagnostics [2, 3], ferrofluid technology [4] and information storage [5]. MNPs are among large number of magnetic nanoparticles, have appeared as a promising candidate due to their   better magnetic properties and biocompatibility [6].   The ratio of surface area to volume of MNPs is very large compared to its bulk magnetite, so these exhibit novel and interesting physical properties [7-9]. These particles below 10 nm in size exhibit superparamagnetic phenomenon, even below its Curie temperature. In this size regime each particle is considered to be a single magnetic domain. Superparamagnetism permits nanoparticles for magnetizing in the presence of a magnetic field, but not to preserve remaining magnetism in its absence [10-13]. Superparamagnetism does not have the hysteresis at 300 K [14]. Interest in the synthesis of magnetic nanoparticles of uniform size and definite morphology has been grown enormously in the recent years due to their promising applications. The MNPs were prepared by modified optimal coprecipitation method in aqueous medium. The coprecipitation method has been studied for more than two decades. The problems in the preparation of MNPs by this method are still present such as, controlling of the particle size, size distribution and particularly the final phase of the required product. Maghemite, hematite and the other iron oxides may be formed due to slight variation in the reaction parameters during the magnetite synthesis process. The objectives of this research study were to optimize the coprecipitation method for the preparation of magnetite without any contamination of other iron oxides and also to study the effects of the synthesis parameters such as stirring rate (rpm *i.e.* revolutions per minute) and reaction temperature on the physical properties of the magnetite particles. These particles were characterized by X-ray Diffractometer (XRD), transmission electron microscopy (TEM), energy dispersive X-ray spectrometer (EDX) and BET surface area analyzer.

Results and Discussion

The solid Iron (III) and Iron (II) salts should entirely new and has not been uncovered to the atmosphere for long time. Iron salts can undertake complex reactions. A number of hydrated Iron (III) salts and Iron (II) salts may dehydrate, but in contrast Iron (III) chloride hexahydrate get moisture on the exposure to the atmosphere. Colour variation specifies whether such reaction have occurred. Iron (III) and Iron (II) solutions should be used promptly after preparation. If Iron (III) solution is kept for some time, then some nucleation of goethite can occur, even at the room temperature. If Iron (II) solutions are kept in open air then it oxidadise to Iron (III).

MNPs were produced by the optimal coprecipitation method. The prevention of air by N_2 gas bubbling was carried out during the entire experiments.   The deionized water and all other solutions, flasks and bottles used in the experiment were purged by N_2 gas. This prevented oxidation of the ferrous ion in the aqueous solution. So the final

---

*To whom all correspondence should be addressed.

phase of our synthetic product was black in colour and possessed strong magnetism which were the characteristics of MNPs.

Fig. 1 and 2 show the XRD and EDX spectrographs of the prepared samples under different reaction conditions. The diffraction peaks of XRD diffractograms of the samples are nearly same to one another and referred to the planes (220), (311), (400), (442), (511) and (440), which were matched well to the JCPDS card 19-0629(synthetic magnetite). The samples were in spinel structure with FCC phase and possessed no contaminations of other iron oxides. The peaks broadening were observed which were due to the small size of the particles.
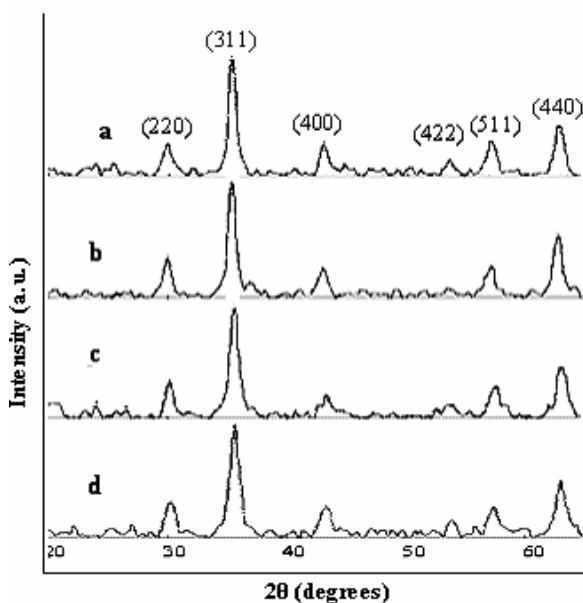

Fig. 1: XRD images of magnetite nanoparticles (samples a – d) produced under different conditions:
(a) 600 rpm, 80 °C, 30 minutes stirring (b) 600 rpm, 60 °C, 30 minutes stirring
(c) 1100 rpm, 80 °C, 30 minutes stirring (d) 600 rpm, 25 °C, 30 minutes stirring

EDX analysis shows that these products are composed of iron and oxygen only. The results reveal that the samples are pure magnetite. The EDX analysis also showed the atomic ratios of the samples

shown in Table-1, are close to the theoretical atomic stoichiometric ratio (42.9% Fe and 57.1% O) for magnetite. The Fe/O ratios are also summarized in the Table-1, for the atomic ratio, which are very near to the theoretical value of magnetite (Fe/O =0.75). The XRD and EDS results showed that the synthesized samples were in magnetite phase.
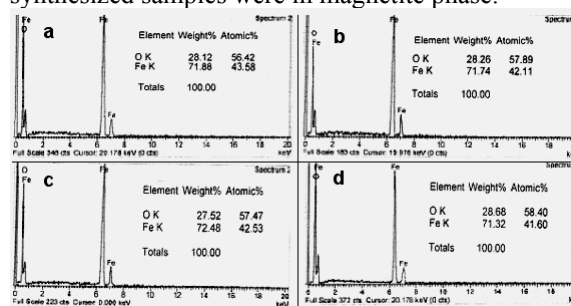

Fig. 2: EDX images of the samples (a)-(d), produced under different conditions as mentioned in Fig. 1.

Table-1: EDX analysis of the prepared samples under different conditions.

Sample No.	Temperature (C°)	Stirring Speed (rpm)	Fe (%)	O (%)	Fe/O (Atomic %)
a	80	600	43.58	56.42	0.7724
b	60	600	42.11	57.89	0.7274
c	80	1100	42.53	57.47	0.7400
d	25	600	41.60	58.40	0.7123

The XRD results also revealed that on increasing temperature, enhances the intensity (crystallinity) of the Bragg peaks of MNPs, hence the full width at half maximum (FWHM) of the peaks decreases. So the particle size of particles increased with increase in synthesis temperature. The XRD results are also compliment with TEM and BET particle size measurements shown in Table-2, where the average particle size was increased as the temperature increased from 25 -80 °C. It was suggested that at the elevated temperature during the synthesis process, the movement of a particle expedited, as a result the volume of the ferrofluid would be expanded and thus its supersaturation would be decreased. The larger particle can be produced at the elevated temperature because at higher temperature, nucleation rate will be slow down and the growth rate will be speed up [15].

Table-2: Comparison of crystal sizes of the prepared particles by XRD, BET and TEM.

S. No.	Temp.(°C)	Stirring (rpm)	2θ (deg)	B_o (deg)	B_i (deg)	B_r (radian)	XRD d(nm)	SA(BET) (m^2/g)	BET d(nm)	TEM d(nm)
a	80	600	35.390	0.6888	0.1570	0.0117	12.41	50.00	23.07	11.66±0.22
b	60	600	35.398	0.7755	0.1570	0.0132	11.02	55.53	20.77	10.31±0.21
c	80	1100	35.420	0.9043	0.1570	0.0155	9.39	104.32	11.06	8.01±0.67
d	25	600	35.430	0.9414	0.1570	0.0162	8.98	110.60	10.43	7.51±0.75

The average crystallite size of the particles of the prepared samples are given in Table-2, was calculated from the full width at half maximum (FWHM) of the major peaks of XRD images with the help of Scherrer formula i.e. $d = K\lambda / B_r Cos\theta_B$ and $B_r = (B_o^2 + B_i^2)^{1/2}$ with d is the thickness of the crystallite, K is constant, dependent on crystallite shape (0.89), λ is x-ray wavelength (0.15405 nm), θ_B is Bragg angle of the major peak and B_r is the real FWHM of the major peak, B_i (B_i = 0.1570nm for standard quartz) is the width due to instrumental broadening effect and B_o is observed FWHM of the major peak of the samples [16].

The particle size of the prepared MNPs was also calculated by the BET and TEM. The particle size via BET method was found from the measured values of surface area of the samples using formula expression, i.e. surface area (SA) = 6/dρ, with diameter of the particle is d and the density of magnetite is ρ (5.20 g/cm^3). Surface area and particle size of the samples are summarized in Table-2. The surface areas of the smaller and greater particles are 110.60 m^2/g and 50.00 m^2/g respectively. The surface area increased with the size reduction of the particles is illustrated in Table-2.

The electron micrographs (Fig. 3) show the morphology of the particles of all samples is spherical. However the particles of the sample (c) & (d) are narrowly distributed. The agglomeration of particles was also observed because they were produced without using any surfactant. The agglomerates produced during the synthesis processes such as decantation and drying, due to higher surface areas of the produced particles.
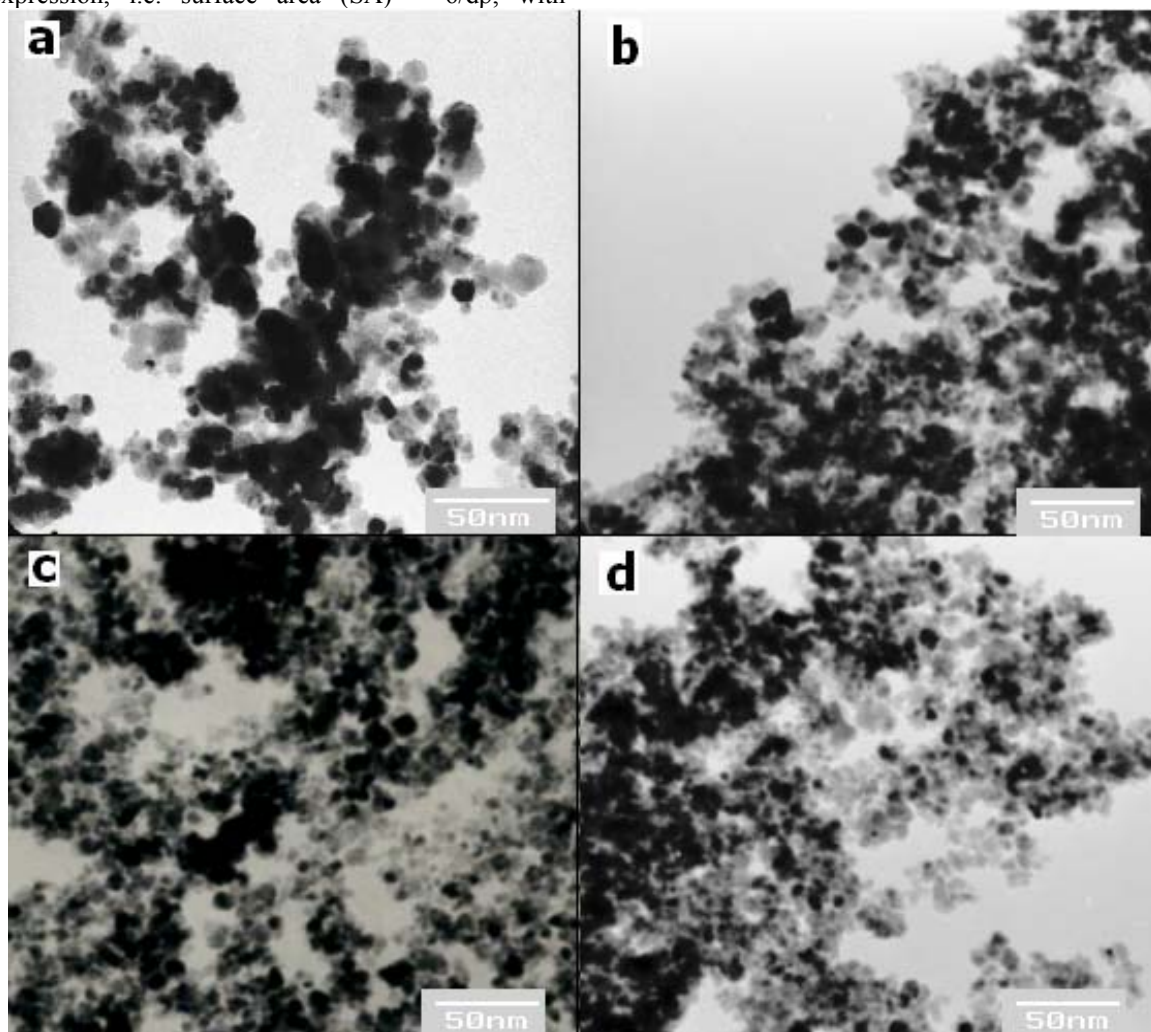

Fig. 3:   TEM images of the samples (a)-(d), produced under different conditions as mentioned in Fig. 1.

The XRD diffractograms (Fig. 1) and TEM electron micrograph (Fig. 3) show when the stirring speed of the reaction system increased from 600 rpm to1100 rpm, under the same temperature and stirring time, the particle size of the samples were reduced, summarized in Table-1 (sample (a)&(c)). The reason of this decreasing of the particle size was suggested that the irregular diffusion of particles at elevated degree of agitation impeded the growth kinetics of the particles, and subsequently produced the particles of smaller size.

The TEM images illustrating the size distribution at various stirring rates are shown in Fig. 3. The particles were agglomerated and their size distribution was broad by stirring the reaction solution at 600 rpm (Fig. 3(a), (b) & (d)). The size distribution was enhanced by stirring the reaction solution at 1100 rpm (Fig. 3(c)). It was suggested that at a low stirring speed the nucleating species are not dispersed uniformly throughout the solution, so the particles are more liable to be agglomerated [17]. Small particles and narrow size particles distribution were achieved due to the enhanced mobility and uniform dispersion of the nucleated species in the reaction solution at higher stirring speed.

It is illustrated in Table-2 that the particle sizes via XRD and BET, are in accord to some extent for the smaller particles (i.e. sample (c) and (d)). However the particle sizes determined from these two techniques do not agree for larger particle size. The crystallite size determined from the XRD line broadening is owing to the coherently scattering volumes of the single crystal grains. Whereas the particle size via BET, calculated from the surface area of the particles which is available for gas adsorption. This might be affected due to the formation of micropores and agglomerates, which do not allow penetrating N_2 gas through it.

Experimental

Materials

All the chemicals were reagent grade and used directly without further purification in the synthesis of MNPs through out the course of this study. The used chemicals were ferric chloride hexahydrate (FeCl$_3$ 6H$_2$O, 99%), ferrous chloride tetrahydrate (FeCl$_2$ 4H$_2$O, 99%), sodium hydroxide (NaOH, 99%) and hydrochloric acid (HCl, 32%) and these were obtained from Alfa Aesar and Scharlau (Germany)

The synthesis was carried out using standard airless process. It was necessary for developing a system that could individually flush out both the iron salt and alkali solution with flow of N_2. Three necks round bottom flask of 500ml and all the other glasswares, used in the experiment, flushed out three times with N_2. The one neck of the round bottom flask was equipped with the N_2 gas pipe, the other was equipped with dropper funnel and the third one equipped with condenser.

Preparation of Solutions for Synthesis of MNPs

All liquids, flasks and bottles were purged with N_2. The entire preparations such as synthesis set up, washing and decantation were performed in the fume hood. All the stock solutions were prepared just before beginning the synthesis process. Deionized water was deoxygenated by bubbling with N_2 gas for 15 minutes prior to use.

i)   150 ml deoxygenated deionized water was transferred in a round bottom flask of 250 ml. The flask was covered with a rubber septum and protected with a cupper wire. The air was degassed from the water with a vacuum pump for 15 minutes and refilled the flask with nitrogen gas. This process was repeated for three times. The arm of the flask was closed soon after filling N_2 gas for the third time.

ii)   9 grams of NaOH pellets were weighed in a round bottom flask of 250 ml and enough deoxygenated deionized water was added for preparing 250 ml of 0.9M NaOH solution. The oxidation protection with N_2 gas flushing was the same as in step (i).

iii) 9.939 grams of FeCl$_2$ 4H$_2$O was weighed in a round bottom flask of 25 ml and degassed the powder for 3 minutes. Enough deoxygenated deionized water was added to the flask for preparing 25 ml of Iron (II) solution. The oxidation protection with N_2 gas flushing in this step was also the same as in the step (i).

iv) 6.7575 grams of FeCl$_3$6H$_2$O was weighed in the other round bottom flask of 25 ml and the pellets were degassed for 3 minutes. The enough deoxygenated deionized water was added to the flask for preparing 25 ml of Iron (III) solution. The oxidation protection with N_2 gas flushing was the same as in the above steps.

Synthesis Growth

i)   4.125ml of FeCl$_2$4H$_2$O and 16.5ml of FeCl$_3$6H$_2$O solutions were mixed in three necks bottle which was already purged three times with N_2 gas.

ii) 250 ml of sodium hydroxide solution was added drop wise at constant rate (4ml/min) to the mixed iron solution under different temperatures and stirring for various samples such as (a) 80 ^{o}C, 600rpm, (b) 60 ^{o}C, 600rpm, (c) 80 ^{o}C, 1100rpm and (d) 25 ^{o}C, 600rpm. Nitrogen gas was passed through the solution in the three necks bottle during the experiment for avoiding the oxidation of Fe^{2+}.

iii) The solutions were heated at the same temperature (specific for the sample as mentioned in the above step) for 30 minutes in order to transform the iron hydroxide into magnetite.

(IV) Crystal Purification

i) The black precipitate was cooled down to the room temperature and pH was near to 12. The three necks bottle was placed in the glove bag filled with N_2 gas.

ii) Then, the obtained product in the flask was separated, by placing on the top of a permanent magnet for enhancing the settling speed. The supernatant was decanted after settling the particles at bottom of the flask.

iii) The precipitate after the first decantation was washed with deoxygenated deionized water and the supernatant discarded after settling the particles. The product was redispersed in the water.

iv) The washing and decantation processes were repeated until to get pH of 7 of the product solution. Subsequently the product was rinsed three times with ethanol and the resulting product was collected by means of magnetic settling and was dried at 50 ^{o}C in vacuum dryer for 20 hours.

(V) Analytical Techniques

(a) X-Ray Diffraction

The prepared particles were characterized for crystallinity and phase composition by x-ray powder diffraction (Rigaku RAD-B system) over 2θ = 20 to 65° at a scanning rate of 3°/min(step size 0.05^o and step time 1 second) using CuKα radiation (λ = 0.15405 nm). Sample preparation for XRD was relatively simple since the particles were already in a powder form. A small piece of double-sided tape was adhered to a glass slide. The particle powder was then deposited on the top of a glass slide and spread out to cover the specified area of the tape. This step is important in order to ensure that a large enough area will be exposed to the x-rays during data collection.

A spatula is used to press the powders onto the glass slide for not blowing off.

(b) Transmission Electron Eicroscope

A Jeol Model CM12 TEM, working at 100KV accelerating voltage, was used to study the morphology, particle size and particle size distribution of the prepared samples. The samples were dispersed in ethanol with ultrasonic sonicator for 5 minutes and a drop of dispersed sample was sprinkled onto a carbon coated copper grid. It was then left for drying in ambient temperature at least 20 minutes and then kept in the desicator for characterization

(c) BET Surface Area Analyzer

The BET (Nova 2000, Quantachrome Instruments, Boynton Beach, USA) method was used for measuring surface area of the sample and N_2 gas was used as adsorbate. The BET method requires that the sample should be dried and outgassed so that to remove adsorbed water. The mean particle size was estimated using the relation $d = 6/\rho A$, with the density ρ and surface area A.

(d) Energy Dispersive X-Ray Spectrometer

The elemental composition of the sample was analyzed with Energy dispersive X-ray spectrometer (EDX). The dispersed particles were sprinkled onto double sided sticky tape which was mounted on a microscopic stub of aluminum.

Conclusion

MNPs can be easily produced from the solution of ferrous/ferric mixed salt-solution in alkaline solution without using any surfactant. The particle size of MNPs increased with the increase in reaction temperature, and decreased with the increase of stirring rate of the reaction system. The size distribution and morphology of the particles improved with increasing in stirring rate. Thus, by restricting the kinetics of nucleation and growth processes through synthesis parameters such as stirring speed and synthesis temperature, the desired particle size and the other properties of the produced particles can be modified according to definite uses.

Acknowledgements

References

1. D. K. Kim, M. Mikhaylova, F. H. Wang, J. Kehr, B. Bjelke, Y. Zhang, T. Tsakalakos, and M. Muhammed, *Chem. Mater,* **15** 4343 (2003).
2. N. Kohler, C. Sun, J. Wang, and M. Zhang, *Langmuir,* **21**(19), 8858 (2005).
3. T. Suwa, S. Ozawa, M. Ueda, N. Ando, and M. Kitajima, *Int. J. Cancer,* **75**(4), 626 (1998).
4. L. J. Love, J. F. Jansen, T. E. Mcknight, Y. Roh, T. J. Phelps, L. W. Yeary, and G. T. Cunningham, *IEEE ASME Trans. Mechatronics,* **10**, 68 (2005).
5. A. Chakraborty, *J. Magn. Magn. Mater,* **204**, 57 (1999).
6. M. A. Morales, T. K. Jain, V. Labhasetwar, and D. L. Leslie-Pelecky, *Appl. Phys,* **97**, 10Q905 (2005).
7. Y. Zhang, N. Kohler, and M. Zhang, *Biomaterials*, **23**(7), 1553 (2002).
8. N. S. Langeroodi, *Journal of the Chemical Society of Pakistan*, **32**, 125 (2010).
9. F. Bakhtiari, M. Zivdar, H. Atashi, S. Seyedbagheri, *Journal of the Chemical Society of Pakistan*, **32**, 215 (2010).
10. P. Tartaj, M. D. Morales, S. Veintemillas-Verdaguer T. Gonzalez-Carreno, and C. J. Serna, J. Phys. D. *Appl. Phys,* **36**(13), R182 (2003).
11. V. M. De Paoli, S. H. De Paoli Lacerda, L. Spinu, B. Ingber, Z. Rosenzweig, and N. Rosenzweig, *Langmuir,* **22**(13), 5894 (2006).
12. K. S. Kim, and J. K. Park, *Lab. Chip ,* **5**(6), 657 (2005).
13. Q. A. Pankhurst, J. Connolly, S. K Jones, and J. Dobson, *Journal of Physics D. Applied Physics,* **36**(13), R167 (2003).
14. K. Liu, L. Zhao, P. Klavins, F. E. Osterloh, and H. Hiramatsu, *Journal of Applied Physics,* **93**(10), 7951 (2003).
15. I. N. Bhattacharya, J. K. Pradhan, P. K. Gochhayat, and S. C. Das, *International Journal of Mineral Processing*, **65**, 109 (2002).
16. H. Klug, and L. Alexander, X-ray diffraction procedures, John Wiley & Sons, Inc., New York p. 491 (1962).
17. S. B. Prabu, L. Karunamoorthy, S. Kathiresan, and B. Mohan, *J. Mater. Process Tech*., **171**, 268 (2006).